Trans Indian Inst Met (2021) 74(8):1917–1922
https://doi.org/10.1007/s12666-021-02279-6

ORIGINAL ARTICLE

# Assessment of Grain Size and Grain Refinement Efficiency by Calculation of Released Heat Attributed to Formation of Primary Aluminum Crystals During Solidification of Al7Si4Cu Alloy

**Aleksandar M. Mitrašinović[1,2] · Dejan B. Momčilović[3] · Zoran Odanović[3]**

Received: 18 June 2020 / Accepted: 26 April 2021 / Published online: 27 May 2021


**Abstract** Assessing heat released only related to the formation of primary crystals provides results with a significantly higher sensitivity than a traditional assessment of undercooling value. In this work, two similar Ti5B1 master alloys (commercial and refined) are used for grain refinement of Al7Si4Cu aluminum alloy to assess narrow differences in heat release during primary crystallization. The heat released related to primary crystallization is $2.50 \pm 0.03$, $3.16 \pm 0.12$, and $7.92$ kJ kg$^{-1}$ for samples treated with the refined master alloys, commercial master alloys, and sample solidified without grain refinement, respectively. The acquired results showed that the suggested method is more efficient in comparison with traditional metallographic or undercooling methods for the assessment of grain refining efficiency with the potential to extend the suggested approach on a wide range of metallic structures where solidification occurs by eutectic-type primary crystallization characteristics.

**Keywords** Grain refinement · Thermal analysis · Heat release · Aluminum · Solidification · Latent heat

**List of Symbols**

| | |
|---|---|
| T | Temperature |
| $T_{Liq}$ | Liquidus temperature |
| $T^{\alpha Al}_{Min}$ | The lowest temperature during primary crystallization |
| $T^{\alpha Al}_{Rec}$ | Recalescence temperature |
| $T^{\alpha Al}_{Start}$ ($T_{Liq}$) | Formation of the first nucleation sites |
| $T^{\alpha Al}_{End}$ | Finalization of primary Al crystals formation and growth |
| $\Delta H^{\alpha\text{-}Al}$ | Heat released from the solidified primary Al crystals |
| $\Delta T^{\alpha Al}_{Undercooling}$ ($T^{\alpha}_{Rec} T^{\alpha}_{Min}$) | Primary undercooling |
| $L^{\alpha Al}$ | Latent heat for primary Al crystals formation |
| $C_p$ | Specific heat |
| t | Time |
| $t^{\alpha Al}_{Rec}$ | Recalescence time ($T^{\alpha Al}_{Min}$–) |
| $t_{Total}$ | Primary crystals formation time ($T^{\alpha Al}_{Start}$–$T^{\alpha Al}_{End}$) |
| $t_{Liq}$ | Time at primary solidification begins |
| $t^{\alpha Al}_{End}$ | Time at primary solidification ends |
| $\left(\frac{dT}{dt}\right)_{CC}$ | Mathematical expression of cooling curve's first derivative |
| $\left(\frac{dT}{dt}\right)_{NC}$ | Mathematical expression of the cooling curve's first derivative without phase transformation |
| CLN | Refined master alloy |
| WCM | Commercial master alloy |
| NC | Newtonian base line |
| CC | Cooling curve |

✉ Aleksandar M. Mitrašinović
alex.mitrasinovic@utoronto.ca

[1] Department of Materials Science and Engineering, University of Toronto, Toronto, Canada

[2] Institute of Technical Sciences of the Serbian Academy of Sciences and Arts, Belgrade, Serbia

[3] Institute for Testing of Materials - IMS Institute, Belgrade, Serbia

## 1 Introduction

Computational methods are effective in simulating heat exchange and mass transfer during solidification processes where input and process parameters are well-established [1–3]. However, in a practical application, there is a demand for immediate access to key process parameters where input materials or surrounding conditions may vary significantly. Establishing a quality control procedure independent of the variations of the input and process parameters and capable of estimating the final structure based on data during the initial stages of solidification would improve the properties of the final products and significantly increase capacities for the producers utilizing solidification processes.

Most studies related to the heat released during solidification consider heat loss from the top surface of the liquid metal contained in the refractory vessel [4–6]. The heat loss from the top creates thermal convection in the liquid alloy. The developed negative thermal gradient from the top to the bottom and sufficiently high thermal undercooling induces the beginning of the solidification from the top of the liquid melt. During solidification, Rayleigh–Benard convection becomes a major force in the bulk below the solid–liquid interface until the entire alloy solidifies [7–9]. Furthermore, the theoretical considerations of the eutectic-type alloys have to incorporate the continuously increasing solid fraction that is dispersed in a liquid. Therefore, a large number of mathematical models have been developed assuming a linear relationship between the solid fraction and the temperature [10] or methods based on the equilibrium lever rule (Scheil equation [11, 12]) and back diffusion [13, 14]. However, neither of these methods is applicable in complex solidification processes, e.g., involving microsegregation [15], volume change [16], multi-component materials [17], or grain refinement [18, 19]. Properties of the final products and producers' capacities would significantly increase if someone develops a technique capable of estimating the final structure based on data during the initial stages of solidification [20].

The main goal of this work is to suggest an advanced in situ method for assessing grain size in solidified Al-Si-Cu alloy that has the potential to replace a widely applied metallographic or undercooling approach. The lower heat released during primary crystallization causes smaller undercooling that further generates large number of nuclei particles that finally results in a finer microstructure. Therefore, monitoring heat release attributed only to the formation of primary aluminum crystals allows estimation of the grain size with an order of magnitude of higher sensitivity than reading undercooling value. Furthermore, assessing heat released values provides correlation to grain size in a solidified structure even for processes where undercooling did not occur. Parameters such as liquidus, primary undercooling and recalescence transitional points were recorded with a K-type thermocouple and data acquisition system and used to quantify the chemical effectiveness of the master alloy during the grain refinement period.

## 2 Experimental Details

A cylindrical stainless steel cup with 5 cm inside diameter and 0.08 cm wall thickness was positioned into the groove of the high-temperature resistant foam (Fig. 1). Either 0.5 or 1.0 g of the Ti5B1 master alloy was placed at the bottom of the stainless steel cup. Then, molten Al-Si-Cu alloy was poured inside the stainless steel cup followed by immediate insertion of K-type thermocouple into the middle of the molten metal. The inoculation period was set at a relatively short period (60 s) to simulate the solidification process where the master alloy was injected into the stream of liquid metal during its pouring into the mold. Thermal analysis recording with the frequency of 50 readings per second was conducted by the National Instruments data acquisition system linked to a personal computer. Liquidus temperature and undercooling were assessed immediately from the cooling curve and its first derivative while other parameters were deduced from the recorded data. Metallographic grain size measurements were done by ASTM E112 standard [21].

The chemical composition of the secondary Al7Si4Cu alloy is given in Table 1 while the specifications of the master alloys are given in Table 2. All master alloy samples met TP-1 international standards [[22]]. Samples marked as WCM are commercial Ti5B1 master alloy used in the automotive industry that often contains a considerable amount of salts and oxides. Samples marked as CLN are refined master alloys with reduced amounts of salts and oxides. The concentrations of Ti and B in CLN samples were also reduced due to the refining process.

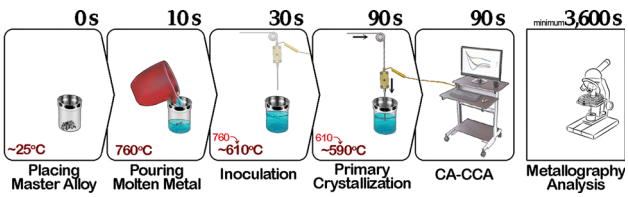


**Fig. 1** Schematics of the grain refinement procedure. (1) Placing master alloy at the bottom of the stainless steel cup, (2) pouring aluminum alloy, (3) immersing thermocouple into the liquid alloy, and (4) recording temperature history during solidification process by the data acquisition system

**Table 1** Chemical composition (wt%) for the Al7Si4Cu alloy measured by the optical emission spectroscopy (OES)

| Si | Cu | Fe | Mg | Mn | Zn | Ti | Ni | Sn | Pb | Al |
|---|---|---|---|---|---|---|---|---|---|---|
| 7.77 | 3.48 | 0.42 | 0.17 | 0.25 | 0.18 | 0.12 | 0.04 | 0.04 | 0.008 | Rest |

**Table 2** Chemical compositions of the master alloys with metallographic characterization of the $TiAl_3$, $TiB_2$ agglomerates larger than 20 μm and oxides larger than 50 μm

| | Chemical composition, wt% | | | | | | $TiAl_3$ | | $TiB_2 > 20$ μm counted particles | Oxide films > 50 μm counted particles |
|---|---|---|---|---|---|---|---|---|---|---|
| | Ti | B | Fe | Si | K | Other | Max Size, (μm) | Avg. Size, (μm) | | |
| ASTM TP-1 standard [[22]] | 4.5–5.5 | 0.9–1.5 | 0.30max | 0.20max | n/d | < 0.10tot | n/d | n/d | n/d | n/d |
| WCM -Ti50B99 | 4.95 | 0.99 | 0.13 | 0.06 | 0.07 | < 0.10tot | 100 | 40 | 4 > 50 μm | 3 > 400 μm |
| WCM -Ti50B96 | 5.02 | 0.96 | 0.14 | 0.08 | 0.06 | < 0.10tot | 90 | 40 | 2 > 35 μm | 1 > 300 μm |
| WCM -Ti50B10 | 5.02 | 1.00 | 0.13 | 0.06 | 0.07 | < 0.10tot | 110 | 40 | 1 > 20 μm | 6 > 600 μm |
| CLN -Ti48B86 | 4.77 | 0.86 | 0.12 | 0.07 | 0.10 | < 0.10tot | 110 | 45 | n/f | 3 > 300 μm |
| CLN -Ti46B83 | 4.62 | 0.83 | 0.12 | 0.06 | 0.09 | < 0.10tot | 105 | 45 | n/f | 1 = 200 μm |
| CLN -Ti45B81 | 4.51 | 0.81 | 0.12 | 0.06 | 0.10 | < 0.10tot | 120 | 45 | n/f | n/f |

*n/d* not defined, *n/f* not found

## 3 Results

Image analysis of the solidified samples (Fig. 2) reveal that after adding 0.5 g of the master alloy into the Al7Si4Cu aluminum alloy, grain size decreases from 1172 (sample without grain refinement treatment) to about 350 μm. Among the same type of samples, higher concentrations of titanium and boron result in lower grain size. Furthermore, alloys solidified after the addition of 1.0 g master alloys have a lower grain size than samples where only 0.5 g of the master alloy has been added (Table 3).

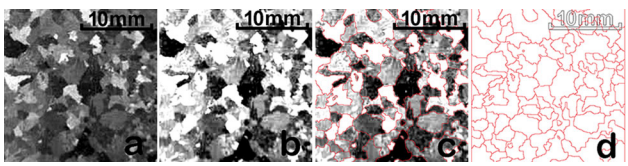


**Fig. 2** Grain size assessment executed by ImageJ software. **a** Light optical image of the aluminum alloy solidified without grain refiner, **b** sharpened 8bit image, **c** detected edges, and **d** determined grain boundaries

### 3.1 Assessment of the Released Heat During Primary Crystallization by Computer-Aided Cooling Curve Analysis

With the advancements in the monitoring techniques in high-temperature conditions, the Computer-Aided Cooling Curve Analysis (CA-CCA) has become the main source of reliable data in assessing solidification parameters in modern metal casting processes. Figure 3 shows a segment of the cooling curve and its first derivative (*dT/dt*) in the area of primary aluminum crystals formation for alloy solidified without adding master alloy. While undercooling and recalescence values can be read directly from the cooling curve, the beginning (liquidus) and the end of primary nucleation are identified from the first derivative curve.

Primary undercooling values range from 0.15 °C for refined alloys up to 0.32 °C for commercial alloys while for sample solidified without refinement, it is 2.83 °C. While the recalescence period is slightly shorter, between 6.3 and 6.8 s, the liquidus and recalescence temperatures in samples treated with refined master alloy are significantly higher in comparison with samples treated with commercial master alloy. Table 4 is summarized key grain refinement parameters obtained from the cooling curve.

The baseline of the cooling curve is generated using the Newtonian method where a few data points are selected

**Table 3** The average grain size of 300 g solidifying alloy treated with Ti5B1 master alloy

| Added master alloy, g | Grain size, μm | |
|---|---|---|
| | Al7Si4Cu (WCM) | Al7Si4Cu (CLN) |
| 0 | 1172 ± 0 | |
| 0.5 | 413 ± 38.89 | 399 ± 1.41 |
| 1.0 | 351 ± 7.21 | 334 ± 8.89 |

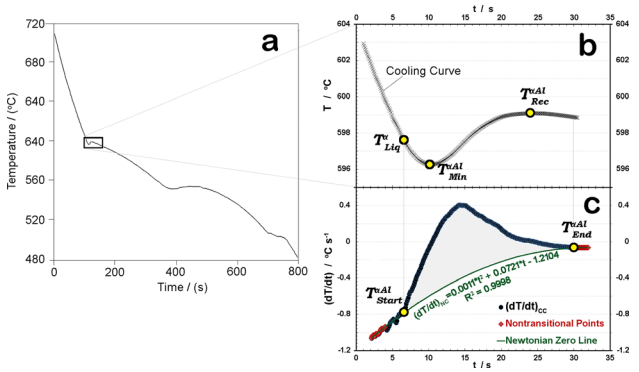


**Fig. 3** The cooling curve of the entire solidification process (**a**), the segment where primary aluminum crystals formation occur (**b**) and the corresponding first derivative (*dT/dt*) of the non-treated Al-Si-Cu alloy with an area corresponding to released heat (the area between *dT/dt* and Newtonian zero line) (**c**). Note: Dots on the diagram show each temperature recording and corresponding *dT/dt* calculation and therefore due to high recording frequency (50 recordings per second) may appear as continuous curves

before liquidus and after all primary aluminum crystals are formed and fitted on the first derivative curve using second-order polynomial equation (Fig. 3, nontransitional points). The baseline represents the shape of the cooling curve first derivative in case phase transformation didn't occur. The released heat is calculated by assessing an area between the cooling curve's first derivative and baseline:

$$\Delta H^{\alpha' Al} = C_p^{Al} \int_{t_{Liq}}^{t^{\alpha Al}_{End}} \left( \left( \frac{dT}{dt} \right)_{CC} - \left( \frac{dT}{dt} \right)_{NC} \right) dt, [kJkg^{-1}] \quad (1)$$

Precise calculations of released heat depends on accurate construction of the baseline (*NC*) and a proper choice of specific heat ($C_p$). Since baseline calculation is done only between liquidus and dendrite coherency point (rather than between liquidus and solidus) where only primary aluminum crystals are formed, the specific heat value is approximated as the value of solid aluminum, 0.904 kJ $kg^{-1}$ $K^{-1}$. While results for both undercooling and heat released correspond in a similar order, a heat released method is capable of detecting much smaller differences in solidification parameters. Among all tests, the samples treated with the refined master alloy have the lowest area between the cooling curve and baseline first derivatives and therefore the lowest heat release (Fig. 4). The heat release is in the range between 2.47 and 2.53 kJ $kg^{-1}$ for samples treated with the refined master alloys while 3.04 to 3.28 kJ $kg^{-1}$ is calculated for samples treated with commercial mater alloy. Alloys solidified without grain refinement release approximately three times more heat (7.92 kJ $kg^{-1}$) in the same solidification conditions.

The area between the first derivative and corresponding baseline characterizes heat released from solidified primary aluminum crystals ($\Delta H^{\alpha\text{-}Al}$). Figure 3 shows that $\Delta H^{\alpha\text{-}Al}$ is significantly higher for alloys solidified without grain refinement while alloys treated with refined master alloy have about 25% lower $\Delta H^{\alpha\text{-}Al}$ than alloys treated with commercial master alloy ($\Delta H^{\alpha\text{-}Al}{}_{NoGrainRefinement} > > \Delta H^{\alpha\text{-}Al}{}_{WCM} > \Delta H^{\alpha\text{-}Al}{}_{CLN}$).

## 4 Discussion

Formation of the solid structure in metallic materials during free cooling begins with the activation of the nucleation sites and subsequent formation of the primary grains. In aluminum, these nuclei become primary crystals and

**Table 4** Parameters obtained from the cooling curves corresponding to primary crystallization of 300 g Al7Si4Cu alloy treated with 1.0 g of Ti5B1 master alloy

| | Master Alloy | $T_{Liquidus}$ (°C) | $T^{\alpha Al}{}_{Min}$ (°C) | $\Delta T^{\alpha Al}{}_{Undercooling}$ (°C) | $t^{\alpha Al}{}_{Rec}$ (s) | $t_{Total}$ (s) | $\Delta H^{\alpha\text{-}Al}$ (kJ $kg^{-1}$) |
|---|---|---|---|---|---|---|---|
| | No Grain Refinement | 598.43 | 596.27 | 2.83 | 13.80 | 26.9 | 7.92 |
| WCM | Ti50B99 | 600.73 | 598.13 | 0.22 | 8.00 | 24.1 | 3.04 |
| | Ti50B96 | 601.24 | 598.27 | 0.32 | 6.70 | 25.1 | 3.22 |
| | Ti50B10 | 599.27 | 597.70 | 0.22 | 7.60 | 23.8 | 3.28 |
| CLN | Ti48B86 | 602.85 | 600.72 | 0.17 | 6.30 | 26.7 | 2.53 |
| | Ti46B83 | 602.23 | 600.95 | 0.15 | 6.30 | 27.6 | 2.51 |
| | Ti45B81 | 602.50 | 600.73 | 0.18 | 6.80 | 28.4 | 2.47 |

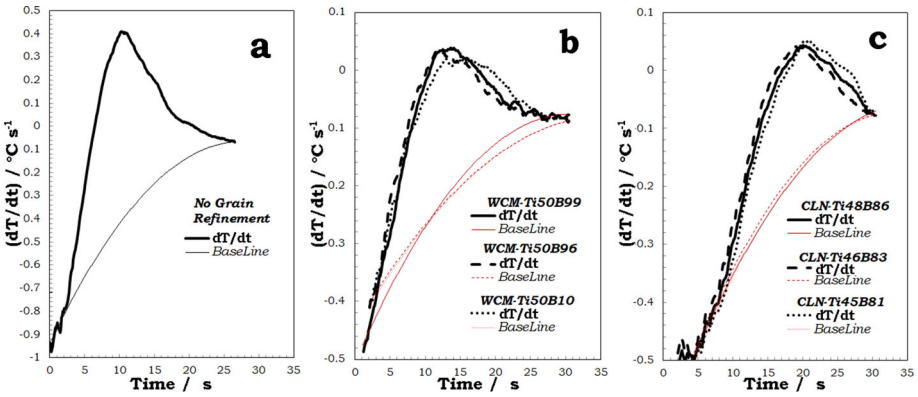


**Fig. 4** The first derivative and baseline curves during primary crystallization of the Al7Si4Cu alloy solidifying without adding master alloy (**a**), after adding 1.0 g of the commercial master alloy (**b**), and after adding 1.0 g refined master alloy (**c**). $\Delta H^{\alpha\text{-}Al}_{NoGrainRefinement} > > \Delta H^{\alpha\text{-}Al}_{WCM} > \Delta H^{\alpha\text{-}Al}_{CLN}$

further by growing to form dendritic structure [23]. Hence, at the moment when neighboring primary crystals impinge each other, the crystal growth stops. However, a large space in between dendritic branches of the primary crystals is filled with remaining liquid [24]. In different samples, the heat released due to the formation of the primary crystals will depend on the amount of the solidified portion of the ratio between solid and liquid phase at the moment when dendritic branches of neighboring crystals impinge on each other. The total heat released for the samples made of the same material will be similar at the end of the solidification process but the rate of the heat released during solidification will differ if these samples are treated differently during the solidification process [25, 26].

During solidification, the heat released by the solidifying microconstituents can be deduced from the cooling curve and its calculated derivatives. These values can be further correlated to the microstructure in the solidified alloy and further microstructure can be correlated to the mechanical properties of the final product. The particulars in the shape of the cooling curve are directly related to various microstructural characteristics. The slopes of the first derivative curves immediately after liquidus temperature are lower in alloys treated with the refined master alloy. This indicates a low initial growth of primary grains and a longer time for the further formation of nuclei. The combination of the lower initial slope and about three seconds longer total time for primary crystals formation before the alloy reaches dendrite coherency point, allows a larger number of smaller grains to form. If we approximate that mass of initial nuclei is negligible to the mass of crystals formed around and that these crystals predominantly consist of aluminum, then the calculated area between the *dT/dt* derivative curve and baseline constructed between liquidus and recalescence temperatures allows for quantitative comparisons of the heat released during primary aluminum crystals formation and growth.

With the rise of computational modeling and the accuracy of new techniques, the classical approach in interpreting solidification parameters needs to be revisited [27–31]. The direct measurement of the grain size in aluminum alloys is difficult to use. Therefore, quantifying the grain size is commonly done by recording the primary undercooling value on the cooling curve. Assessing primary undercooling has a disadvantage in cases where adding more master alloy causes primary undercooling values approach zero and further assessment of grain refinement efficiency by primary undercooling criterion would be difficult. In addition to primary undercooling, the recalescence period, cooling rate, and liquidus temperature can be easily recorded and read from the same cooling curve. These parameters allow for the calculation of released heat.

Figure 5 provides comparisons between the heat released during the formation of the primary aluminum crystals and primary undercooling values. Since the calculation of heat released during phase transformation is the sum of temperatures over the set time, the sensitivity of the method is much higher than assessing only undercooling temperature. Reports focusing on released heat for the entire solidification process found similar results regardless alloy grain refinement is employed or not. However, this work focuses on the area around primary crystals formation where the significant differences in released heat can be distinguished.

The assessments of the grain refining efficiency heavily rely on the properties of the thermocouples. While digital readings of the thermocouples could be displayed with seemingly very high accuracies in practical applications, sensitivity step for either K or J type thermocouples is around 0.01 °C. With the increased efficiency of grain refinement, the undercooling values are smaller and therefore sensitivity of the particular method reduces. In some cases, undercooling does not appear on the cooling curve. However, assessment of the realized heat provides

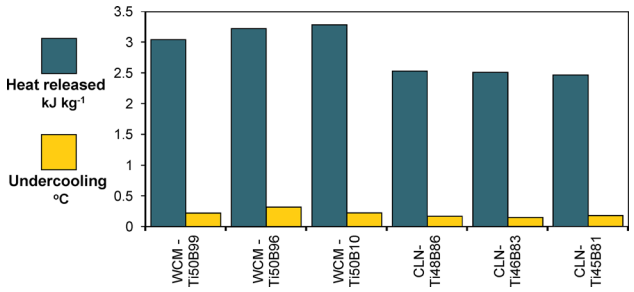


**Fig. 5** Comparison between primary undercooling and heat released in Al7Si4Cu alloy after adding 1 g Ti5B1 master alloy

valuable data regarding grain refining efficiency, grain size, and other important parameters that are deducible from the alloys' solidification history even in cases where undercooling did not occur. Further improvement in assessing the grain size by calculating released heat should include temperature dependent values of specific heat ($C_p^{Al}$) [32] that will further increase the method's sensitivity.

## 5 Conclusions

Taking into consideration, the heat released during primary solidification of the Al7Si4Cu alloy was demonstrated to be the most advanced in situ method for assessing the microstructure in the solidified sample that further could be correlated to the mechanical properties of the final product. The difference in liquidus, primary undercooling, and recalescence temperatures were investigated in the Al7Si4Cu aluminum alloy solidified without grain refining and alloy treated with the Ti5B1 master alloys. The thermal analysis technique allowed in situ estimation of the grain size in the solidified structure where assessing heat released during formation of the primary aluminum crystals in the Al7Si4Cu aluminum alloy was an order of magnitude more sensitive than the undercooling criterion.

**Acknowledgements** Authors would like to express their appreciation to Dr. Robin Francis for his assistance in conducting experiments and members of the UW IRC in Light Metal Casting Technology for their valuable advice and support. The support of the Ministry of Education, Science and Technological Development, the Republic of Serbia (Record #: 451-03-68/2020-14/200175 and ON172005) is also kindly acknowledged.

## References

[1] Campbell J, *Complete Casting Handbook, Metal Casting Processes, Techniques and Design*, Elsevier Ltd., Butterworth-Heinemann (2011), 187–390. https://doi.org/10.1016/C2011-0-04123-6
[2] Lazaridis A A, *Int. J. Heat Mass Transfer* **13** (1970) 1459.
[3] Horr A M, *Computational Evolving Technique for Casting Process of Alloys, Mathematical Problems in Engineering*, Article ID 6164092, 2019; https://doi.org/10.1155/2019/6164092
[4] Fadl M, and Eames P C, *Applied Thermal Engineering* **151** (2019) 90.
[5] Palacz M, Melka B, Wecki B, Siwiec G, Przylucki R, Bulinski P, Golak S, Blacha L, and Smolka J, *Metals and Materials International* **26** (2020) 695.
[6] Kathait D S, *International Research Journal of Engineering and Technology*. **03** (2016) 1627.
[7] Ostrogorsky A G, and Glicksman M E, *Segregation and Component Distribution. Handbook of Crystal Growth: Bulk Crystal Growth*. 2nd ed. Elsevier; Butterworth-Heinemann (2015).
[8] Zürner T, Schindler F, Vogt T, Eckert S, and Schumacher J, *Journal of Fluid Mechanics* **876** (2019) 1108.
[9] Oh J, Ortiz de Zárate J M, Sengers J V, and Ahlers G, *Physical Review*. **E69** (2004) 021106.
[10] Chaung Y K, and Schwerdfeger K, *Arch. Eisenhüttenwes* **44** (1973) 341.
[11] Gulliver G H, *J. Inst. Met*. **9** (1909) 120.
[12] Scheil E, *Ztsch. Metallkunde* **34** (1942) 70.
[13] Won Y M, and Thomas B G, *Metall. Mate. Trans. A*. **32A** (2001) 1755.
[14] Brody H D, and Flemings M C, *Trans. Met. Soc. AIME*. **236** (1966) 615.
[15] Lacaze J, and Lesoult G R J, *Materials Science and Engineering: A* **173** (1993) 119.
[16] Faden M, König-Haagen A, and Brüggemann D, *Energies* **12** (2019) 868.
[17] Fujimura T, Takeshita K, and Suzuki R O, *International Journal of Heat and Mass Transfer* **130** (2019) 797.
[18] Kotadia H R, Qian M, and Das A, *Trans Indian Inst Met* **71** (2018) 2681.
[19] Ren-Guo G, and Di T, *Acta Metallurgica Sinica(English Letters)* **30** (2017); (5) 409.
[20] Czerwinski F, *Metallurgical and Materials Transactions B* **48** (2017) 367.
[21] ASTM Volume 03.01 Metals – Mechanical Testing; Elevated and Low-Temperature Tests; Metallography (2020) ISBN 978–1–6822–1519–7
[22] Standard Test Procedure for aluminium alloy grainrefiners: TP-1 Washington DC, USA, The Aluminum Association; (1990).
[23] Nampoothiri J, Raj B and Ravi K R, *Trans Indian Inst Met* **68** (2015) 1101.
[24] Böttger B, Carré A, and Eiken J. et al., *Trans Indian Inst Met* **62** (2009) 299.
[25] Fardi-Ilkhchy A, Binesh B, and Shaban Ghazan, M, *Trans Indian Inst Met* **72** (2019) 2319.
[26] Chen Y, Feng Y, and Wang L et al., *Trans Indian Inst Met* **72** (2019) 533.
[27] Quested T E, *Materials Science and Technology* **20** (2004) 1357.
[28] Jiang B, Qiu D, Zhang M X, Ding P D, and Gao L, *Journal of Alloys and Compounds* **492** (2010) 95.
[29] Jacques L, Béchet E, and Kerschen G, *Finite Elements in Analysis and Design* **127** (2017) 6.
[30] Saruyama Y, Tatsumi S, and Yao H, *Polym. Int.* **66** (2017) 207.
[31] Ghomashchi R, and Nafisi S, *Journal of Crystal Growth* **458** (2017) 129.
[32] Buyco E H, and Davis F E, *J. Chem. Eng. Data* **15** (1970) 518.